

Instability of Equivalent-Barotropic Riders

MARK SWENSON*

Scripps Institution of Oceanography, University of California, San Diego, La Jolla, CA 92093

(Manuscript received 5 June 1986, in final form 20 October 1986)

ABSTRACT

It is shown, by the integration of numerical initial-value problems, that modon-with-rider solutions to the equivalent barotropic equation are unstable in the parametric range relevant to Gulf Stream rings. The fastest growing mode is found to have azimuthal wavenumber 2.

1. Introduction

Gulf Stream rings, when detached from the Gulf Stream, evolve very slowly, are nearly circular, and transport fluid (Richardson, 1983). There is no evidence of forcing on the time and length scales of rings, which suggests that they maintain their coherence through a balance between dispersion and nonlinearity, as in the classical example of the Boussinesq solitary wave. Only two of the many quasi-geostrophic solitary wave models that have been proposed incorporate the basic characteristics of rings: approximate radial symmetry and a region of trapped fluid. One of these (Flierl, 1979) has been shown to employ an invalid asymptotic expansion (Swenson, 1986). The other, first suggested by Flierl (1976), consists of a baroclinic monopole superimposed upon a barotropic dipolar modon (Stern, 1975). Although the stability of the latter solution has not been thoroughly investigated, it appears that it is unstable (McWilliams and Flierl, 1979). Other modon-with-rider solutions have been found (Flierl et al., 1980), however, and the possibility that a one-mode configuration is useful for modeling rings cannot be ignored. In this paper, we examine numerical, initial-value calculations of single-mode modon-with-rider solutions and find them to be unstable. This demonstration, together with the result of Swenson (1986), eliminates the known quasi-geostrophic solitary wave models of rings and thereby directs attention to the importance of either radiation and dissipation or non-quasi-geostrophic effects in ring dynamics.

2. Theory

Modon-with-rider solutions for the equivalent-barotropic equation have been calculated by Flierl et al. (1980), but we present a brief derivation here in

order to establish notation. The conservation of potential vorticity is described by

$$\frac{D}{Dt_*} \left\{ \nabla_*^2 \psi_* + \beta y_* - \frac{1}{r_i^2} \psi_* \right\} = 0, \quad (1)$$

where the asterisks denote dimensional variables, ψ_* is the streamfunction,

$$\frac{D}{Dt_*} \equiv \frac{\partial}{\partial t_*} + \frac{\partial \psi_*}{\partial y_*} \frac{\partial}{\partial x_*} + \frac{\partial \psi_*}{\partial x_*} \frac{\partial}{\partial y_*}, \quad \nabla_*^2 \equiv \frac{\partial^2}{\partial x_*^2} + \frac{\partial^2}{\partial y_*^2},$$

$\beta =$ constant northward gradient of the Coriolis frequency, and $r_i =$ internal deformation radius. We assume that the motion is steady and that the eddy is strong in the sense that it will have a closed streamline region (as viewed from a reference frame attached to the eddy). Together, these assumptions imply that the eddy propagates only in the east-west direction. Transforming (1) to a reference frame moving with the eddy, we find that

$$J_* \left(\psi_* + c_* y_*, \nabla_*^2 \psi_* + \beta y_* - \frac{1}{r_i^2} \psi_* \right) = 0, \quad (2)$$

where c_* is the phase speed of the eddy and $J_*(A, B) \equiv A_x B_y - A_y B_x$. For modons, (2) holds separately for the two regions $r_* \gtrless L$. This implies that the curve $r_* = L$ is a streamline so that

$$\psi_* = \Psi_* - c_* r_* \sin \theta \quad \text{at } r_* = L, \quad (3)$$

where Ψ_* is a constant. Introducing the nondimensionalization $r_* = r_i r$, $c_* = \beta r_i^2 c$, $\psi_* = \beta r_i^3 \psi$, and $\Psi_* = \beta r_i^3 \Psi$, we obtain

$$J(\psi + cy, \nabla^2 \psi - \psi + y) = 0, \quad (4)$$

$$\psi = \Psi - cr \sin \theta \quad \text{at } r = 1, \quad (5)$$

where J is the dimensionless Jacobian operator and we have chosen $L = r_i$ to correspond with the scaling in Flierl et al. (1980). Alternatively, we may consider the first integral of (4)

* Present affiliation: Areté Associates, PO Box 6024, Sherman Oaks, CA 91413

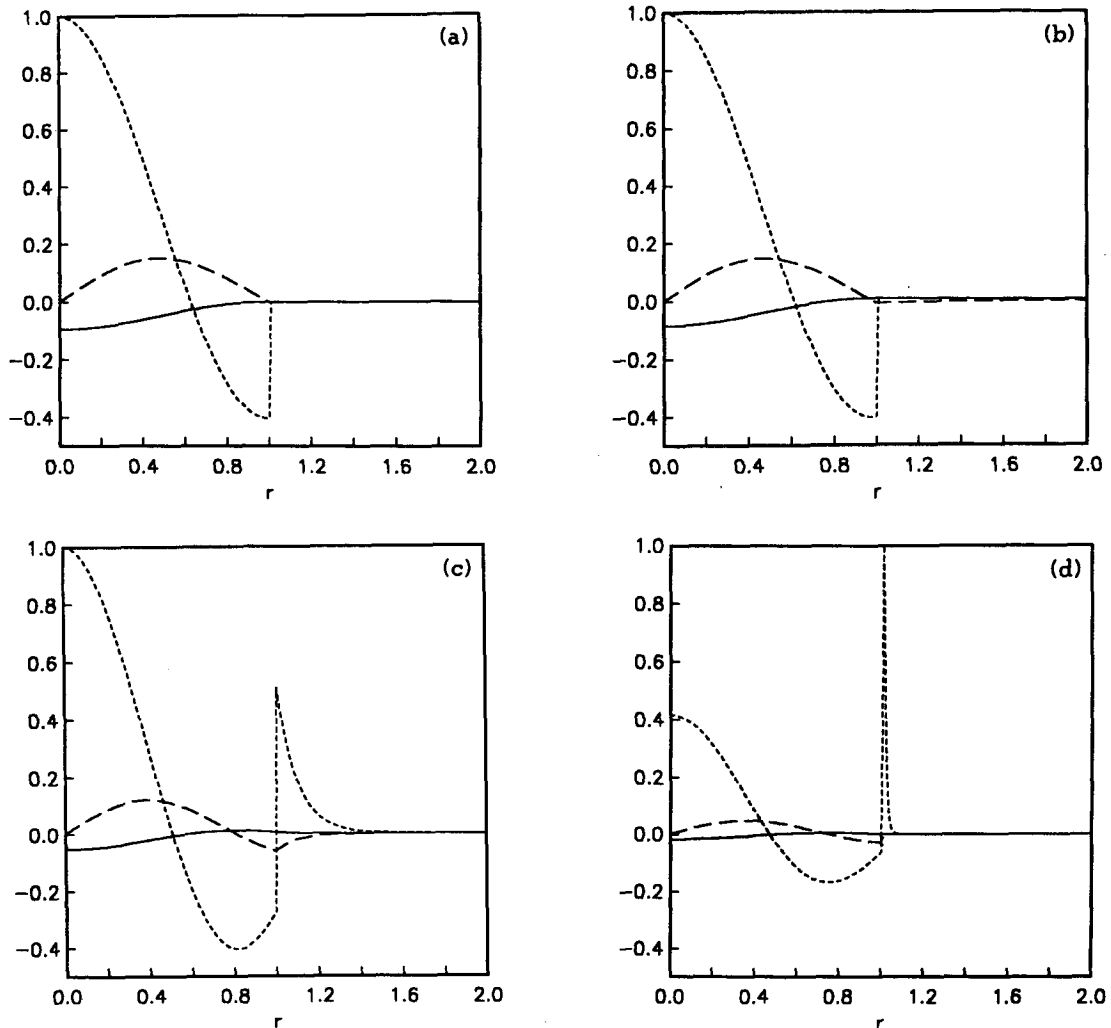


FIG. 1. Radial profiles of streamfunction (solid), azimuthal velocity (long dashed), and vorticity (short dashed) for (a) $q = 0.1$, (b) $q = 1$, (c) $q = 10$, (d) $q = 100$. All have been normalized so that maximum vorticity is 1.

$$\nabla^2 \psi - \psi + y = P(\psi + cy), \quad (6)$$

where P is the (arbitrary) potential-vorticity functional. The modon problem consists of (6), (5) and the condition that the tangential velocity be continuous at $r = 1$.

For $r > 1$, P may be evaluated asymptotically for $r \rightarrow \infty$ to obtain

$$P(X) = \frac{1}{c} X, \quad r > 1. \quad (7)$$

Following Flierl et al. (1980), for $r < 1$ we posit

$$P(X) = \lambda - (k^2 + 1)X, \quad r < 1. \quad (8)$$

Introducing the notation

$$\psi = \psi_R + \psi_M \sin \theta = \begin{cases} \psi_R^> + \psi_M^> \sin \theta, & r > 1 \\ \psi_R^< + \psi_M^< \sin \theta, & r < 1, \end{cases} \quad (9)$$

so that ψ_R represents the rider and $\psi_M \sin \theta$ represents the underlying modon, we may write the solution as

$$\psi_R^> = \Psi \frac{K_0(qr)}{K_0(q)}, \quad (10)$$

$$\psi_M^> = -c \frac{K_1(qr)}{K_1(q)}, \quad (11)$$

Table 1. Summary of stability experiments.

Experiment	c	Rider strength	Duration
A	-2	0	7.8
B	1	0	7.8
C	-2	strong	3.9
D	1	strong	3.9
E	-2	moderate	7.8
F	1	moderate	3.9

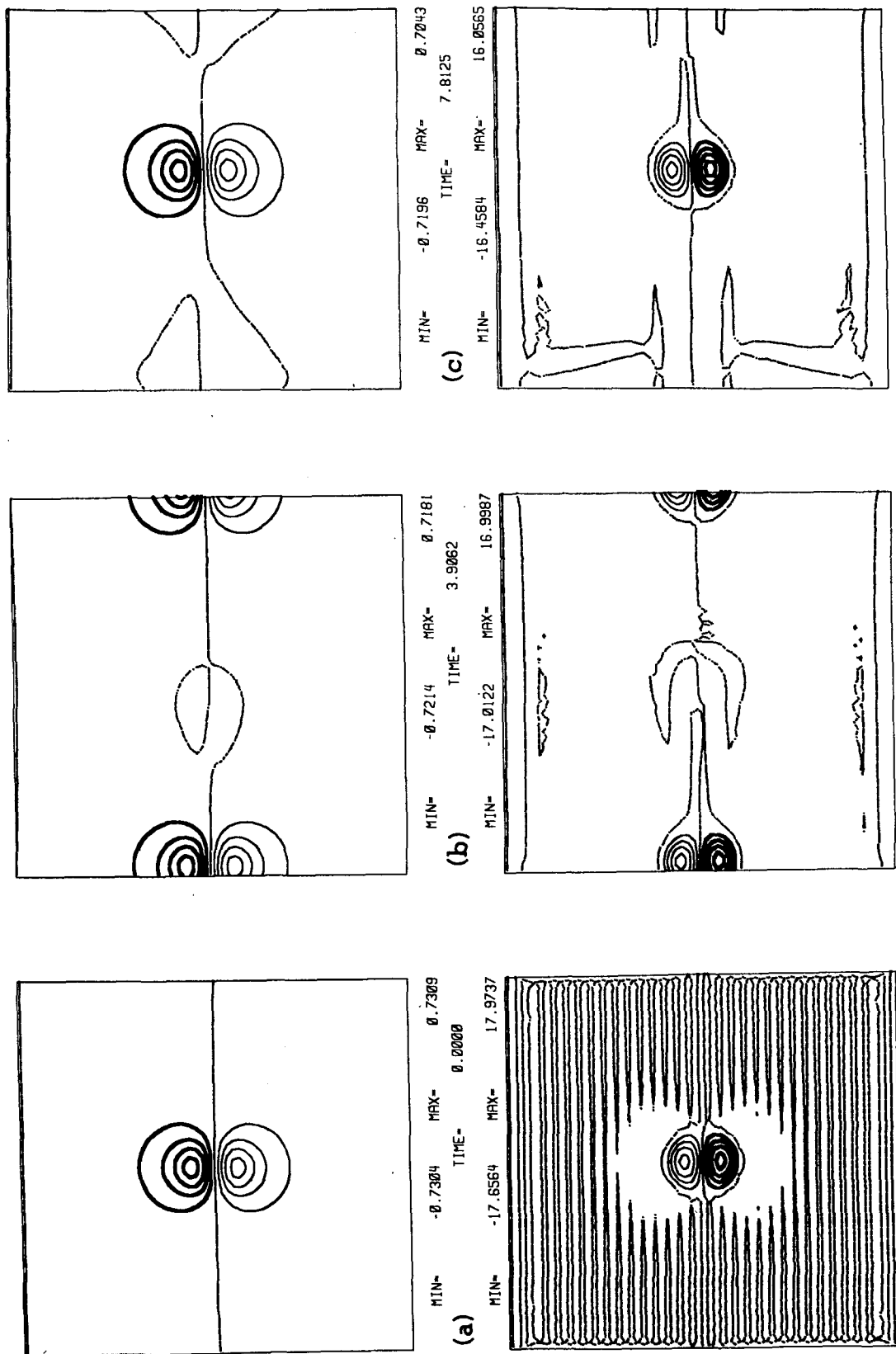


FIG. 2. Time sequence of contour maps for experiment A. Contour intervals are variable. Heavy contours are positive, light contours are negative, and the dotted contour is zero. Upper panel is streamfunction, lower is vorticity.

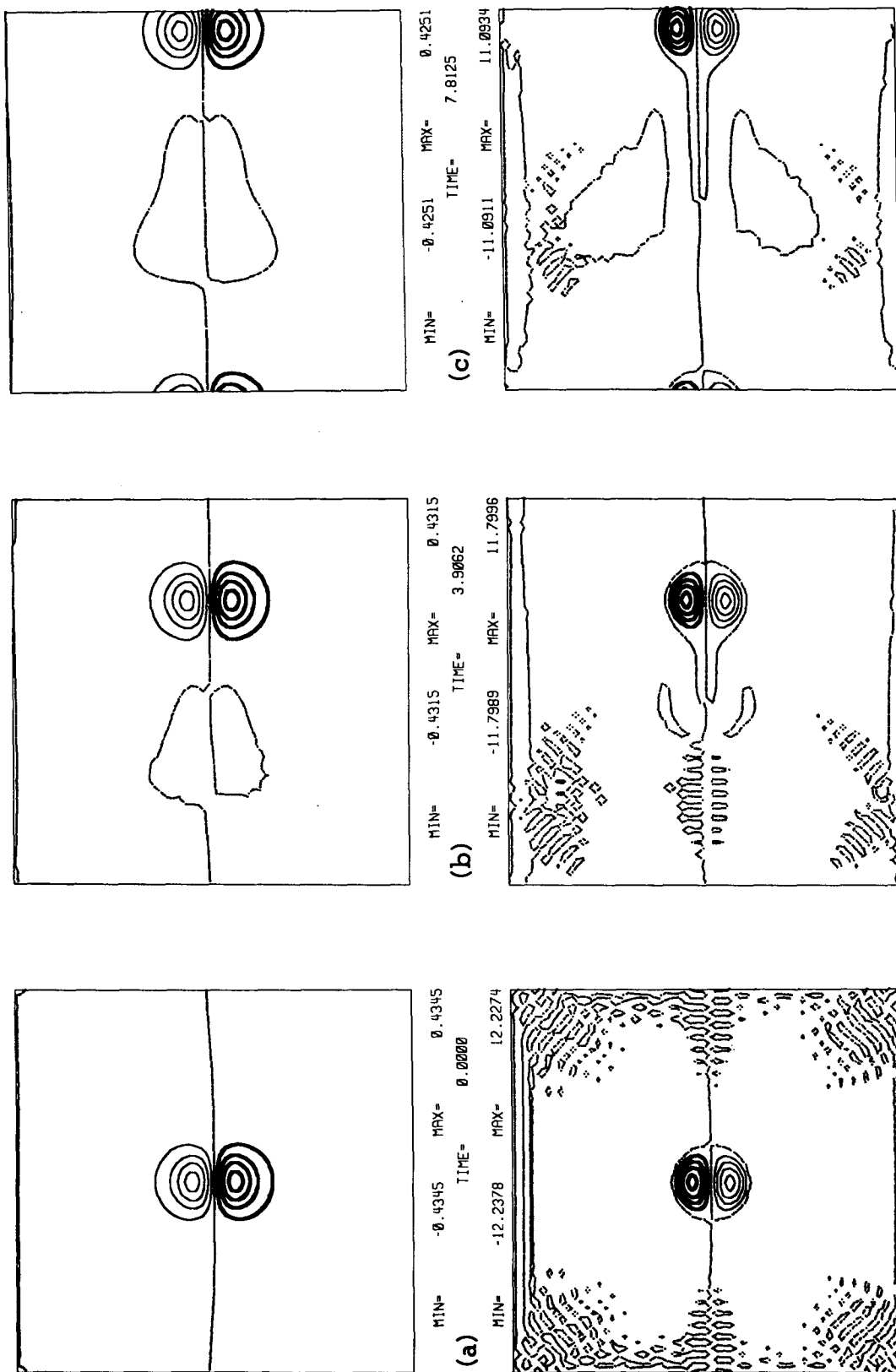


FIG. 3. As in Fig. 2 but for experiment B.

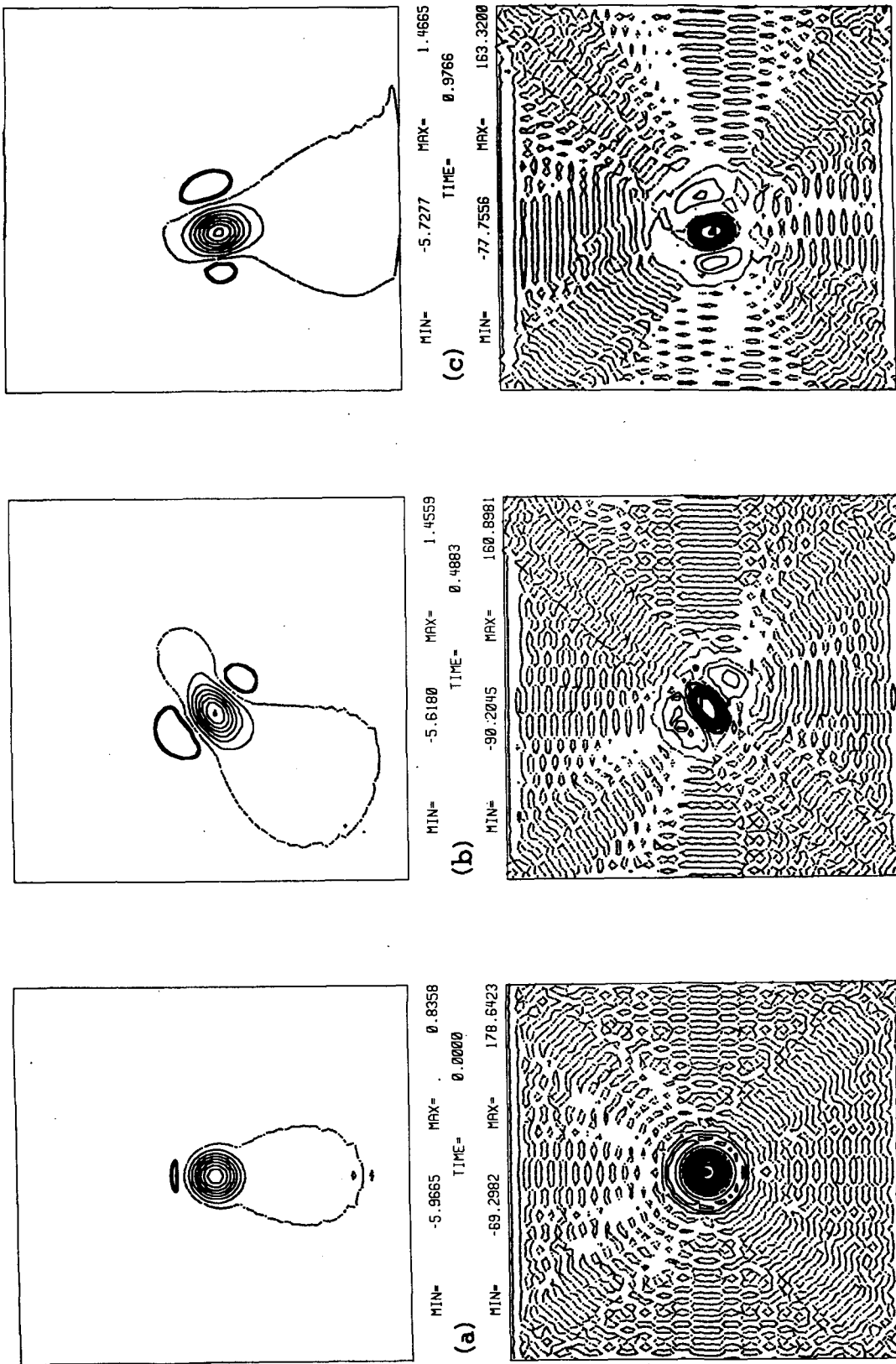


FIG. 4. As in Fig. 2 but for experiment C.

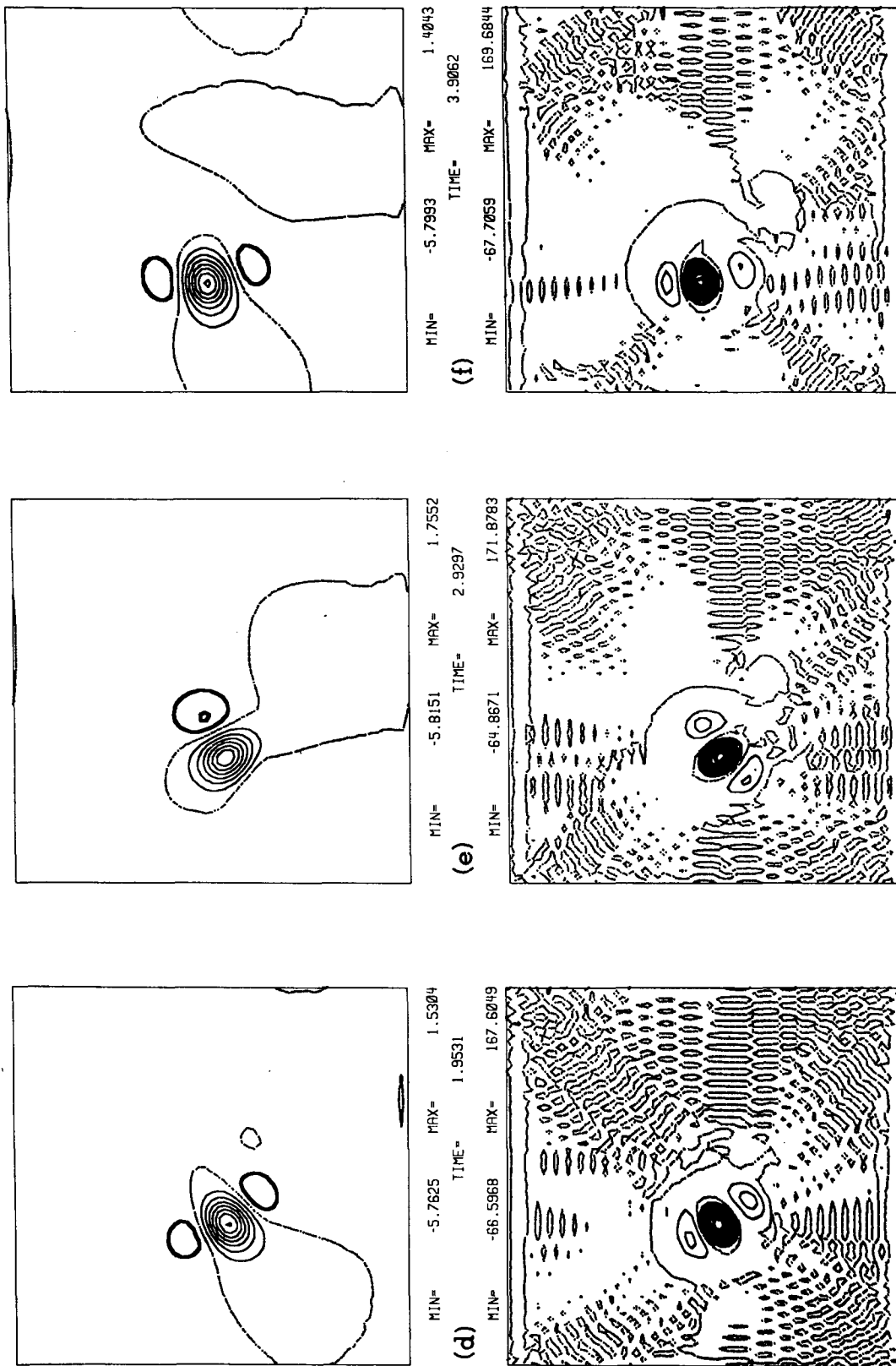


FIG. 4. (Continued)

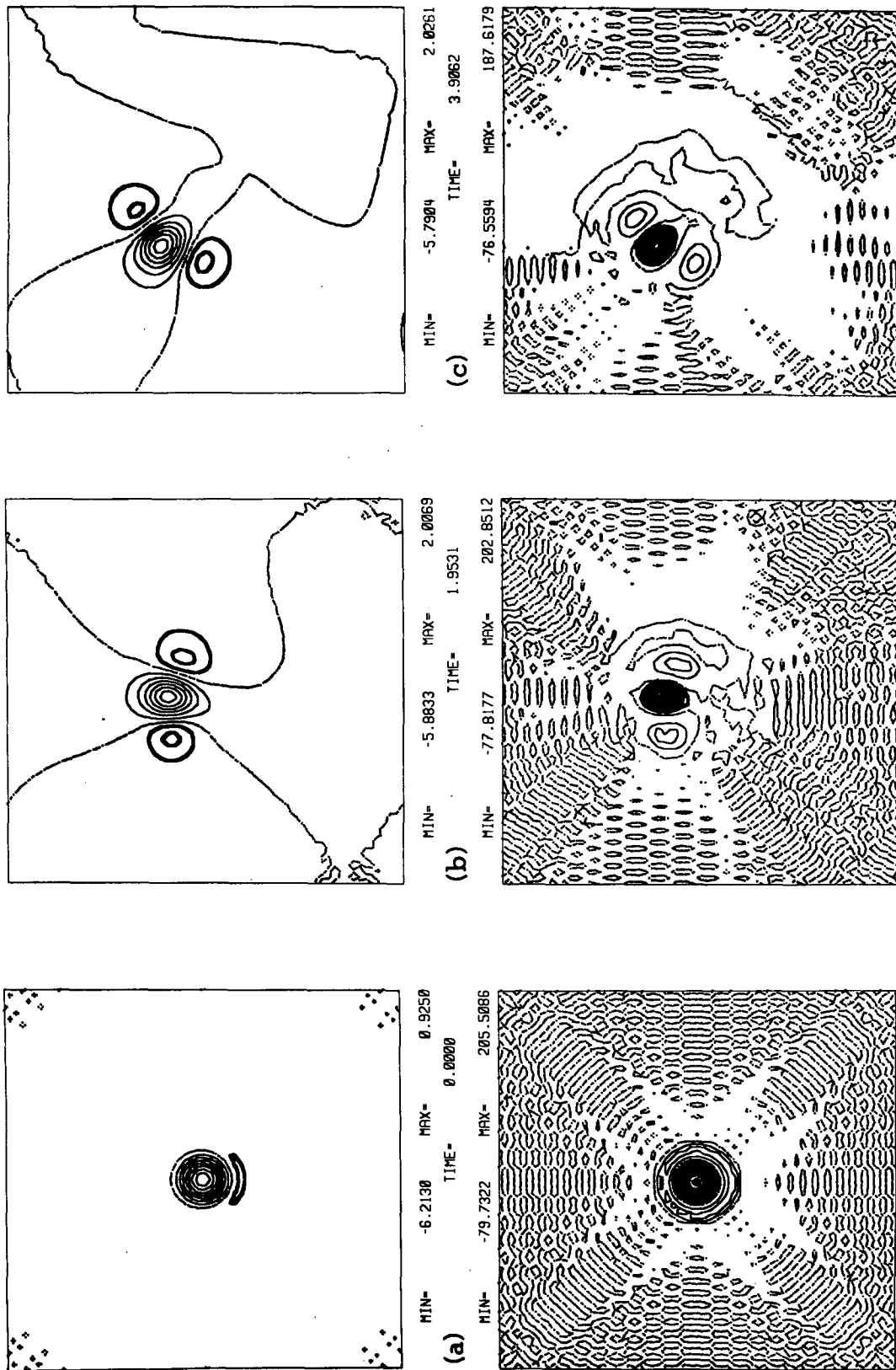


FIG. 5. As in Fig. 2 but for experiment D.

$$\psi_R^< = m\Psi + (1 - m)\Psi \frac{J_0(kr)}{J_0(k)}, \tag{12}$$

$$\psi_M^< = c \left[\frac{q^2 J_1(kr)}{k^2 J_1(k)} - \left(1 + \frac{q^2}{k^2} \right) r \right], \tag{13}$$

where

$$q^2 \equiv 1 + \frac{1}{c}, \tag{14}$$

$$m \equiv 1 + \frac{K_2(q)J_0(k)}{K_0(q)J_2(k)}, \tag{15}$$

$$\frac{K_2(q)}{qK_1(q)} = \frac{-J_2(k)}{kJ_1(k)}, \tag{16}$$

$$\Psi = m^{-1}k^{-2}\lambda, \tag{17}$$

and $c < -1$ or $c > 0$. The addition of the rider imposes a discontinuity in vorticity at the modon boundary:

$$\lim_{\epsilon \rightarrow 0} \nabla^2 \psi|_{r_1+\epsilon}^{r_1-\epsilon} = [k^2(1 - m) + q^2]\Psi. \tag{18}$$

This solution also has the important property that the integrated vorticity vanishes, i.e.,

$$\int_0^{2\pi} \int_0^\infty \nabla^2 \psi r dr d\theta = 0.$$

Radial profiles of ψ_R and $\nabla^2 \psi_R$ are displayed in Fig. 1 for four values of q . For small q , there is very little vorticity outside of the modon boundary, while on the inside there is a positive vortex core surrounded by a negative vorticity ring. As q increases, the distribution of vorticity changes appreciably. A band of positive vorticity is observed just outside of the modon boundary. This band becomes narrower and stronger as q increases. In the limit $q \uparrow \infty$ the vorticity distribution resembles a δ function.

3. Numerical investigation of stability

A conventional analytical investigation of the stability of the modon-with-rider configuration appears to be intractable. The proof of Laedke and Spatschek (1986), which showed that westward-traveling, equivalent-barotropic modons are spectrally stable, cannot be extended to the modon-with-rider. The addition of a non-zero rider introduces a discontinuity in vorticity which implies that Eqs. (73) and (74) of Laedke and Spatschek (1986) no longer represent conserved quantities. Swaters (1986) established sufficient conditions for linear Liapunov stability of equivalent-barotropic modons. Analogous conditions apply to the modon-with-rider configuration, but the conditions do not preclude the instability of the configuration for arbitrary linear perturbations. Therefore, we use numerical

integrations of initial value problems in order to assess the stability of these solutions.

a. The numerical model

We use a pseudospectral numerical method to obtain solutions to

$$\frac{\partial}{\partial t} (\nabla^2 - 1)\psi = -J(\psi, (\nabla^2 - 1)\psi) - \psi_x \tag{19}$$

for specified initial conditions and the periodicity conditions

$$\phi(x, y, t) = \phi(x + 2\pi, y, t) = \phi(x, y + 2\pi, t). \tag{20}$$

The Jacobian terms are evaluated using Orszag's (1971) alias-free, staggered-grid algorithm, which insures exact conservation of energy and enstrophy, while the time integration is accomplished by the centered-difference approximation. In order to prevent instability of the computational mode, the solution is averaged locally in time every 30 time steps, as well as after the initial forward-difference time step. Aside from errors due to initial sampling, time stepping, and round off, the only error of the alias-free scheme is that it disallows interactions with wavenumbers higher than the cutoff, which causes enstrophy to accumulate near the cutoff wavenumber. To alleviate possible problems, we apply a weak, wavenumber-dependent filter (Laplacian friction) at each time step to prevent enstrophy accumulation; this leaves energy virtually unchanged. Except for a slight smoothing of contours, the addition of this friction does not change the results of the numerical integrations.

b. The simulations

The modon-with-rider solutions constitute a family with two independent parameters, the phase speed c and the rider amplitude Ψ . Although rings are observed to move westward about 5 cm s^{-1} on average (Richardson, 1983), the extent to which this is due to self-propulsion is unclear since rings may be advected by large-scale mean flows, which are also characterized by speeds of 5 cm s^{-1} . We therefore examined several cases of both eastward and westward travelling solutions, i.e., we examined $c \in (-2, -1)$ and $c \in (0, 2)$, where $c = 1$ corresponds to a dimensional speed of $\beta r_i^2 \sim 5 \text{ cm s}^{-1}$. The two cases $c = -2$ and $c = 1$ are representative of our results and are discussed in detail in this section. Rider amplitudes are chosen to correspond to a young, energetic ring ($U \sim 140 \text{ cm s}^{-1}$, where U is the characteristic swirl velocity) and an older, less energetic ring ($U \sim 50 \text{ cm s}^{-1}$). (Lower rider amplitudes are of limited physical interest. The formal possibility that the modon-with-rider configuration is stable for rider amplitudes below some threshold value cannot be adequately

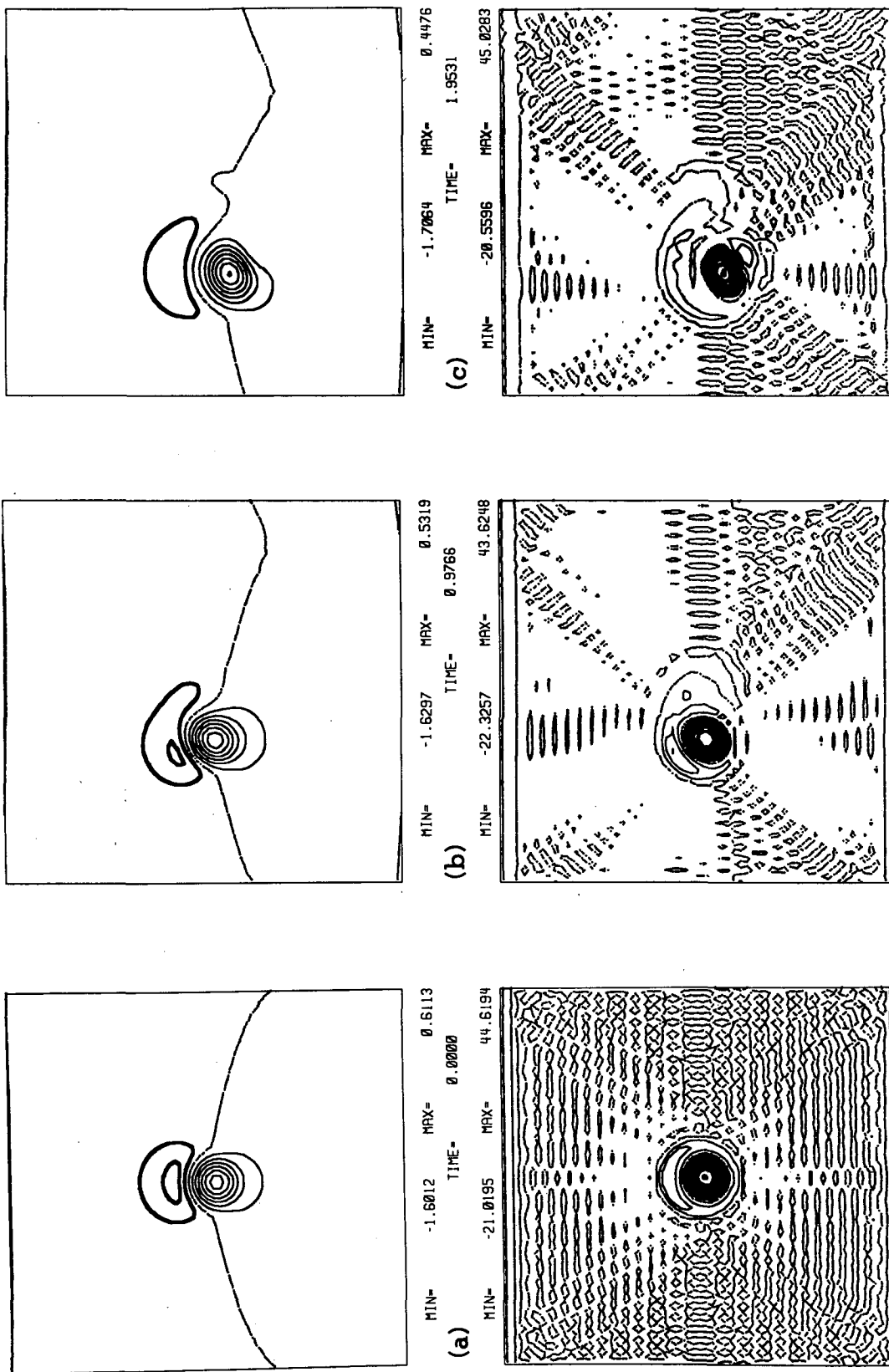


FIG. 6. As in Fig. 2 but for experiment E.

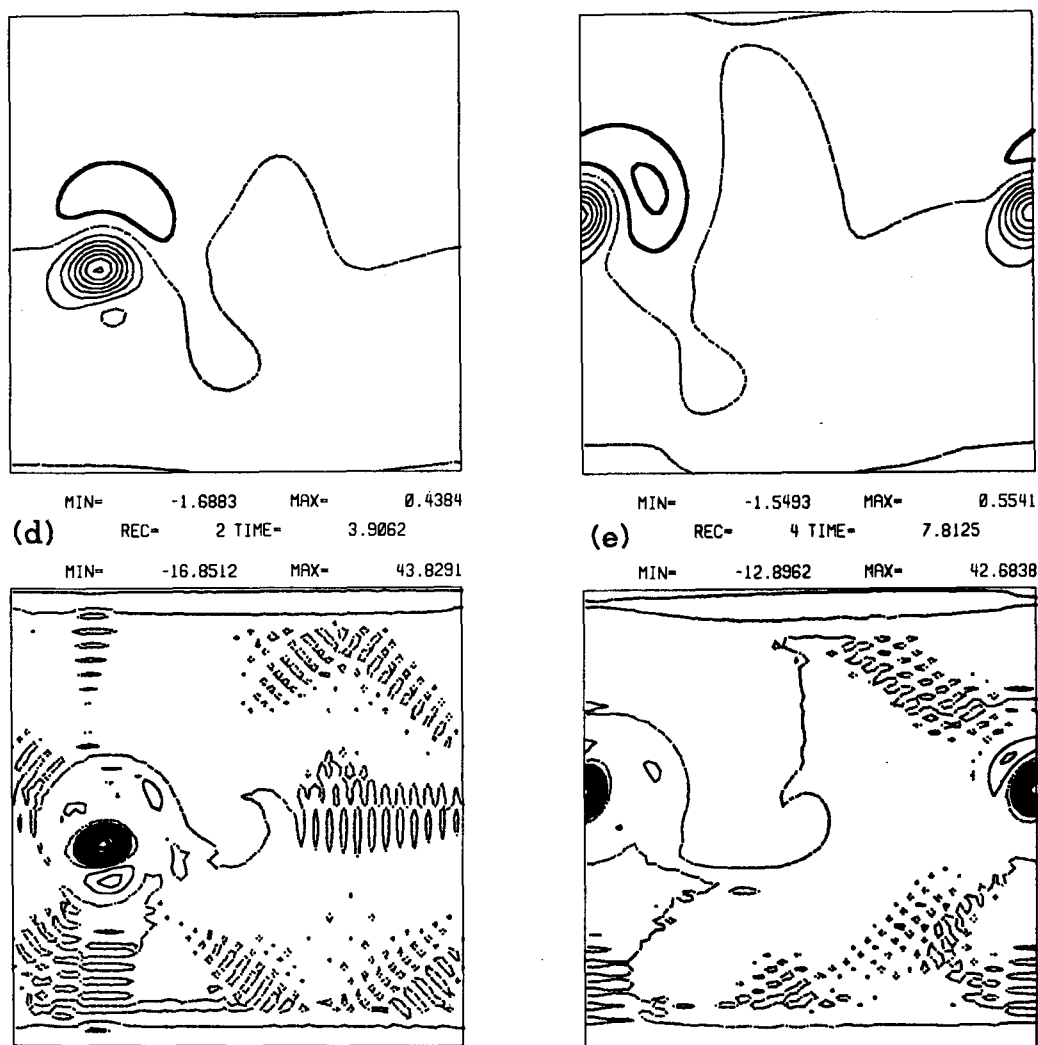


FIG. 6. (Continued)

addressed by the method employed herein.) In addition, to provide a basis for comparison, we present simulations when the riders are absent. The experiments are summarized in Table 1.

The integrations are run for at least 3.9 nondimensional time units, which corresponds to about 1 month. For the integrations presented in this paper, which have a cutoff wavenumber of 32, a corresponding low resolution (cutoff wavenumber 16) experiment also was considered. The reduced resolution did not have significant effects on the results of the integrations.

1) NO RIDER (EXPERIMENTS A AND B)

When the rider is absent, the numerical integration provides a good representation of the modon evolution (Figs. 2 and 3). The numerical phase speeds are about

93% of the analytical value, which compares favorably with the results of McWilliams et al. (1981) for similar resolution.

2) STRONG RIDER (EXPERIMENTS C AND D)

We now consider modon-with-rider solutions where the rider amplitude has been chosen so that typical swirl velocities are about 140 cm s^{-1} (Figs. 4 and 5). This leads to initial conditions that are dominated by the rider. Although the radial profile of the rider changes considerably over the range of interest (eg., $q \uparrow \infty$ as $c \downarrow 0$; see Fig. 1), the evolution of the modon-with-rider for strong riders is similar for all of the cases examined, and differs markedly from the analytically predicted behavior. Instead of propagating uniformly with the appropriate phase speed, the eddy immediately

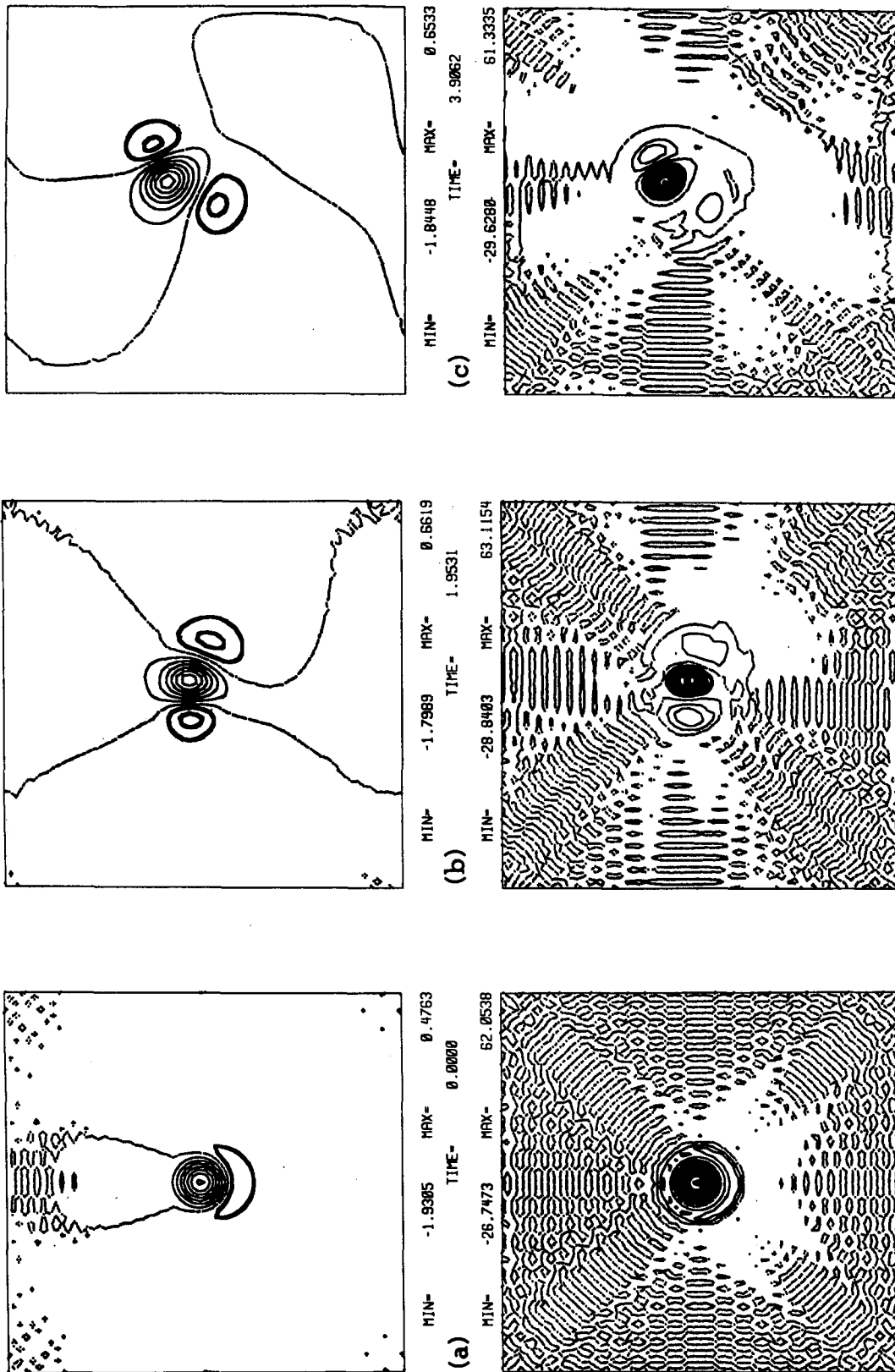


FIG. 7. As in Fig. 2 but for experiment F.

begins to distort owing to the growth of a disturbance with azimuthal wavenumber 2. (See Gent and McWilliams, 1986, for other examples of wavenumber-two barotropic instabilities in vortices.) The result is a characteristic low-high-low vorticity pattern that is reminiscent of the instability of concentric, uniform potential-vorticity patches on the f -plane (Flierl, 1984b). We have conducted numerical experiments that show the similarity between the instability of the rider (alone) on the f -plane and the evolution in experiments C and D. This indicates that, initially, the underlying modon and the β -effect act as perturbations to the rider, which is unstable on the f -plane. After the initial unstable mode growth, the vortices undergo a complicated interaction which differs in detail from case to case.

3) MODERATE RIDER (EXPERIMENTS E AND F)

When the rider is scaled so that typical swirl velocities are about 50 cm s^{-1} , the rider no longer dominates the initial conditions in those cases for which the magnitude of the phase speed is greater than approximately $3/2$. For these cases, the swirl velocity of the underlying modon is relatively large ($U \sim 20\text{--}30 \text{ cm s}^{-1}$), so that the strength of the rider is about equal to the strength of the modon (Experiment E, Fig. 6). Again, we find that the modon-with-rider evolves very differently from the analytically predicted behavior (section 2). Here, the β -effect and the underlying modon influence the evolution even for small times. The mutual advection of the two vortices dominates the evolution initially. Although the low begins to orbit the high immediately, the high propagates in the analytically predicted manner (section 2) for at least a week. Subsequently, the low is sheared apart and weakens steadily as it circulates around the high, which, after the initial westward advection, moves westward at a reduced rate ($c \geq -1$) in a manner similar to a Gaussian vortex (McWilliams and Flierl, 1979).

In experiment F ($c = 1$), the rider dominates the underlying modon even for a rider of moderate amplitude. The evolution (Fig. 7) is qualitatively similar to that for a strong rider (experiment D), except that the two emerging low vortices do not grow to equal size, which indicates that the β -effect and the modon affect the evolution at an earlier stage for moderate riders.

c. Summary

Modon-with-rider solutions are equilibrium solutions of the equivalent-barotropic equation (in a uniformly-translating reference frame). We have shown them to be unstable in the parametric range relevant to Gulf Stream rings. The instability is analogous to

an azimuthal wavenumber 2 instability of concentric potential-vorticity patches on the f -plane (Flierl, 1984b). This is apparent in the calculations with strong riders (Figs. 4 and 5), but the instability is masked by complicated interactions of the dipolar modon, Rossby waves, and the rider and its instabilities when the rider strength and modon strength are commensurate.

4. Comments

The similarity of the instability in the strong rider runs (Figs. 4 and 5) to the instability of two concentric, uniform potential-vorticity patches (Flierl, 1984b) suggests that a detailed analogy would be helpful in understanding the rider instability. In particular, the integrated potential vorticity of riders is zero so that the corresponding theory for concentric patches on the f -plane is very simple. The main result of Flierl's theory for this special case is that the concentric patches are stable if the zero crossing (i.e., radius of inner patch) is less than $1/2$ of the radius of the entire eddy. The zero crossing for riders occurs at $r < 1/2$ for $c \leq 0.0048$, or $q \geq 14.5$. For $q \geq 10$, however, the rider is no longer similar to a two patch configuration because a third band of vorticity exists just outside of the modon radius (Fig. 1). Numerical experiments indicate that this configuration is unstable to an azimuthal wavenumber 2 mode that is similar to the one observed in Figs. 4 and 5.

During the course of investigating the instability of riders (alone) on the f -plane, we observed that the rider for $q = 10$ evolved into two nearly equal vortex pairs (Experiment G, Fig. 8). (We have added a small amplitude, white-noise perturbation field to the initial streamfunction field for this experiment. This speeds up the development of the instability, but does not affect the nature of the evolution.) This adds to the growing evidence that vortex pairs can be generated by unstable vortex flows (Basdevant et al. 1984*; Flierl 1984a, 1985). This example differs from previous ones in its initial condition, which has three bands of alternating vorticity rather than two.

The numerical results presented in this paper eliminate the possibility that known, quasi-geostrophic solitary wave solutions are good models for ring dynamics. Although numerical calculations indicate that the equivalent-barotropic equation admits solutions that are very similar to rings (McWilliams and Flierl, 1979), recent attempts to model ring behavior analytically incorporate non-quasi-geostrophic processes (Flierl 1984a, Charney and Flierl 1981, Matsuma and Yamagata 1982). As theorists begin to grapple with the

* The Batchelor couples referred to by Basdevant, et al. (1984) were obtained by Lamb (1932).

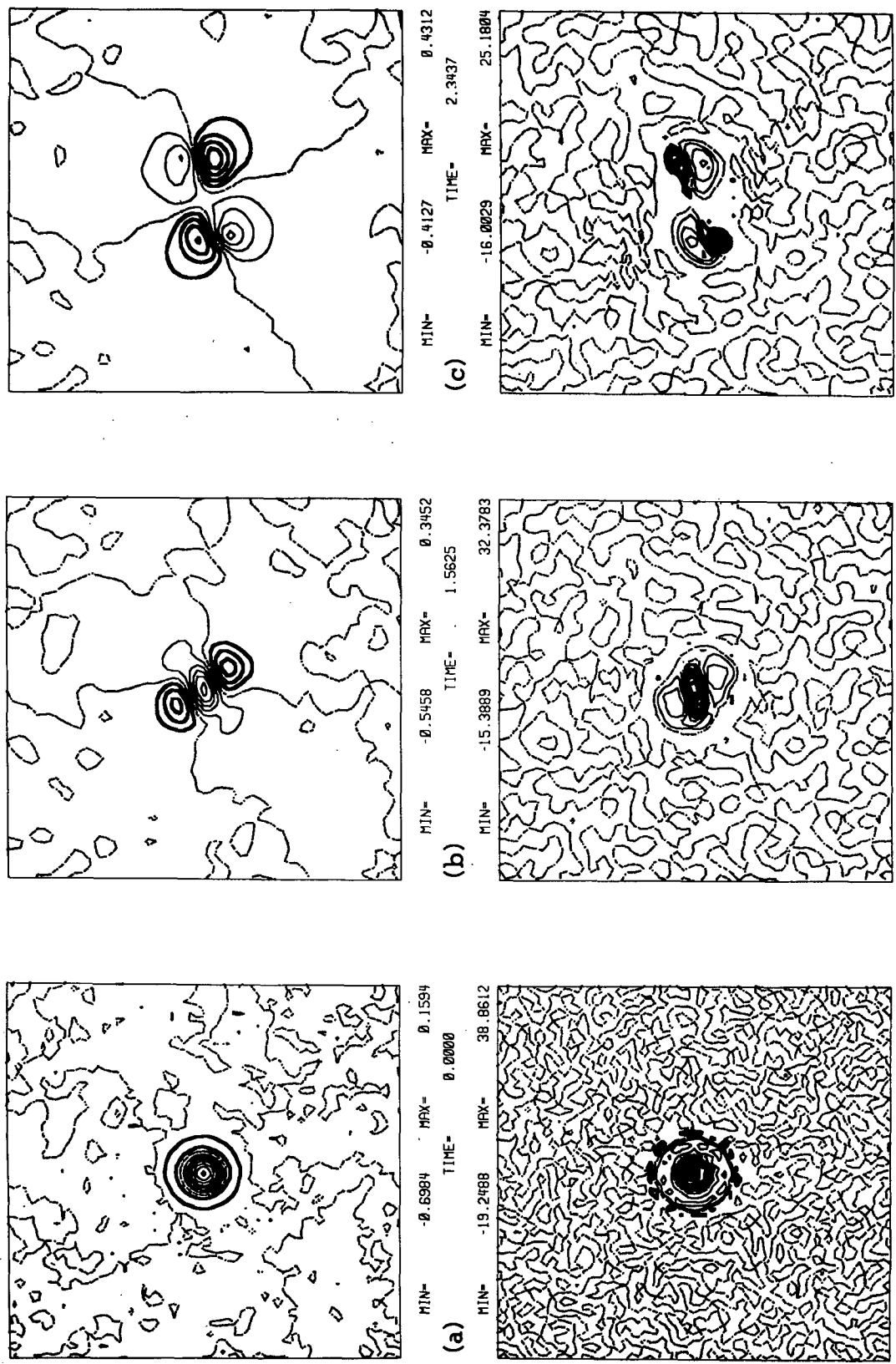


FIG. 8. As in Fig. 2 but for experiment G.

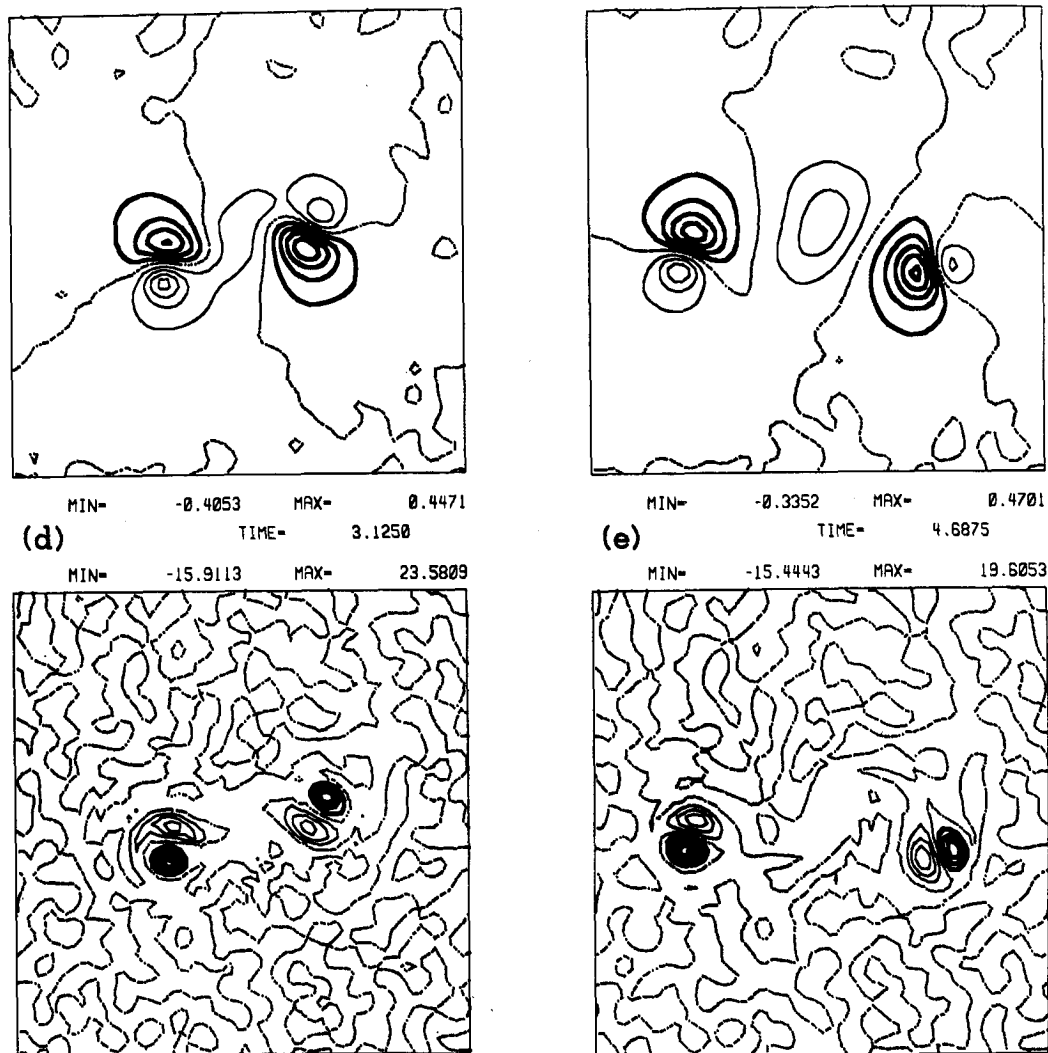


FIG. 8. (Continued)

problems posed by the realistic (i.e., complicated) behavior of rings in the ocean, it will be vital to know if non-quasi-geostrophic effects are important to rings or whether, within the quasi-geostrophic approximation, it is more profitable to explore the effects of radiation, time dependence and dissipation in order to model ring dynamics.

Acknowledgments. I wish to thank Prof. John W. Miles, Prof. Myrl C. Hendershott, Prof. Glenn R. Flierl, Ms. Annalisa C. Griffa and Dr. Arthur J. Miller for many beneficial discussions. Thanks are also due to Prof. Rick Salmon, who kindly provided a code for the Jacobian calculations. This work was supported by NSF Grant OCE-81-17539 and forms part of my Ph.D. thesis.

REFERENCES

- Basdevant, C., Y. Couder and R. Sadourny, 1984: Vortices and vortex-couples in two-dimensional turbulence. *Macroscopic Modelling of Turbulent Flows*, U. Frisch and J. B. Keller, Eds., Springer-Verlag, 327-346.
- Charney, J. G., and G. R. Flierl, 1981: Oceanic analogues of large-scale atmospheric motions. *Evolution of Physical Oceanography*, B. A. Warren and C. Wunsch, Eds., MIT Press, 504-549.
- Flierl, G. R., 1976: *Theory and Modeling of Ocean Eddies: Contributions of the US Delegation to the Yalta POLYMODE Theoretical Institute*. POLYMODE Office, MIT.
- , 1979: Baroclinic solitary waves with radial symmetry. *Dyn. Atmos. Oceans*, 3, 15-38.
- , 1984a: Rossby wave radiation from a strongly nonlinear warm eddy. *J. Phys. Oceanogr.*, 14, 47-58.
- , 1984b: The emergence of dipoles from instabilities on the f - and β -plane. *Woods Hole Oceanogr. Inst. Tech. Rep.*, WHOI-84-44, 104-110.

- , 1985: Instability of vortices. Woods Hole Oceanogr. Inst. Tech. Rep., WHOI-85-36, 119–121.
- , V. Larichev, J. McWilliams and G. Reznik, 1980: The dynamics of baroclinic and barotropic solitary eddies. *Dyn. Atmos. Oceans*, **5**, 1–41.
- Gent, P. R., and J. C. McWilliams, 1986: The instability of barotropic circular vortices. *Geophys. Astrophys. Fluid Dyn.*, **35**, 209–233.
- Laedke, E. W., and K. H. Spatschek, 1986: Two-dimensional drift vortices and their stability. *Phys. Fluids*, **29**, 133–142.
- Lamb, H., 1932: *Hydrodynamics*. Cambridge University Press, §165.
- McWilliams, J. C., and G. R. Flierl, 1979: On the evolution of isolated, nonlinear vortices. *J. Phys. Oceanogr.*, **9**, 1155–82.
- , ——, V. Larichev and G. Reznik, 1981: Numerical studies of barotropic modons. *Dyn. Atmos. Oceans.*, **5**, 219–238.
- Matsuma, T., and T. Yamagata, 1982: On the evolution of nonlinear planetary eddies larger than the radius of deformation. *J. Phys. Oceanogr.*, **12**, 440–456.
- Orszag, S., 1971: Numerical simulation of incompressible flow within simple boundaries. *Stud. Appl. Math.*, **L**, 293–327.
- Richardson, P. L., 1983: Gulf Stream rings. *Eddies in Marine Science*, A. R. Robinson, Ed., Springer-Verlag, 19–45.
- Stern, M., 1975: Minimal properties of planetary eddies. *J. Mar. Res.*, **33**, 1–13.
- Swaters, G. E., 1986: Stability conditions and a priori estimates for equivalent-barotropic modons. *Phys. Fluids*, **29**, 1419–1422.
- Swenson, M. S., 1986: A note on baroclinic solitary waves with radial symmetry. *Dyn. Atmos. Oceans*, **10**, 243–252.